J Fluoresc (2012) 22:1639–1645
DOI 10.1007/s10895-012-1108-3

ORIGINAL PAPER

# Structural and Upconversion Studies of $Er^{3+}$ Codoped with CdS Nanoparticles in Sol-Gel Glasses

**L. Bokatial · S. Rai**

Received: 30 May 2012 / Accepted: 30 July 2012 / Published online: 8 August 2012


**Abstract** The $Er^{3+}$ codoped with CdS nanoparticles in sol-gel glass with an average particle size of about 10 nm have been synthesized by sol-gel method. The green and red up-conversion emissions centered at about 534, 560 and 680 nm, corresponding to the $^2H_{11/2}\rightarrow{}^4I_{15/2}$, $^4S_{3/2}\rightarrow{}^4I_{15/2}$ and $^4F_{9/2}\rightarrow{}^4I_{15/2}$ transitions of $Er^{3+}$, respectively; were detected by a 800 nm excitation**.** The two-photon absorption process is involved in the green and red up-conversion emissions.

**Keywords** Sol-gel chemistry · Nanoparticles · Glasses · Electron microscopy · Luminescence

## Introduction

In the recent years, the upconversion of infrared light to shorter wavelength by rare-earth ions doped glasses have been investigated extensively, due to wide applications such as high density optical data storage, solid state color display, infrared sensor, optoelectronics, sensitive bioprobes and underwater sea communications [1–4]. $Er^{3+}$ ion is the most studied among the rare earth ions, and the upconversion process of this ion in various kinds of host materials has been investigated [5–13]. Upconversion (UC) requires the absorption of two or more photons but unlike the multiphoton absorption, the photons can be absorbed sequentially rather than simultaneously. A condition for efficient UC pumping is that the absorbing center has a metastable state that is intermediate in energy between the ground state and the emitting state. UC lasing has several advantages over other techniques such as second harmonic generation.

To convert the fundamental infrared emission to the visible, non-linear optical techniques such as harmonic generation or optical parametric oscillation are generally employed. There are several stringent conditions relating to the infrared beam quality, beam divergence, polarization orientation, crystal temperature and crystal axis alignment that must satisfied when using non-linear methods. Poor conversion efficiency will result if these conditions are not met. In contrast, UC laser emission is an effective means of converting IR radiation to the visible without many of the constraints associated with NL optical techniques [14, 15].

However, the glasses with lower phonon energy can lead to higher UC efficiency. Among oxide glasses, tellurite glasses have been proven to be with lower phonon energy than many oxide glasses [16]. Unfortunately, silicate glasses which are the most chemically and mechanically stable and also are easily fabricated into various shapes and size such as rod and optical fiber have only vary faint UC luminescence due to their large phonon energy [17]. Therefore design of new silicate glass host for realizing intense UC luminescence from $Er^{3+}$ is target at present. Semiconductor nanocrystals have received much attention due to their size-dependent optical properties of these nanoparticles make them unique materials for a variety of applications. Several advantages could result from co-doping matrices with nanoparticles and rare earth (RE) ions. It is known that the absorption bands of nanoparticles are broader than those of RE which ensures the accord ability in wavelength of the pump sources for the achievement of optical components such as amplifiers. An appropriate choice of the semiconductor nanoparticles would then lead to excite the rare-earth ion by nonradiative energy-transfer between the semiconductor nanoparticles and the rare-earth ion through the matrix [17]. CdSe, CdTe and CdS nanocrystals, are the group of nanostructures that have been mostly investigated

L. Bokatial
Department of Physics, Dibrugarh University,
Dibrugarh, 786004 Assam, India
e-mail: ltlbktl@gmail.com

S. Rai (✉)
Department of Physics, Mizoram University,
Aizawl, 796004 Mizoram, India
e-mail: srai.rai677@gmail.com

because of their high luminescence efficiency and easily adjustable luminescence from ultraviolet to near infrared region by nanocrystals sizes showing the prospective for optoelectronic devices and biological imaging and labeling applications [17–21].

In the present study, the nonradiative decay rates of excited $Er^{3+}$ ions and up conversion mechanism of $Er^{3+}$ in CdS nanoparticles under 800 nm excitation are considered mainly from the CdS concentration dependence. Intensity parameters of optical transitions of $Er^{3+}$ in silicate glasses codoped with CdS nanoparticles are calculated from absorption spectra using Judd-Ofelt (J-O) theory.

## Experimental

Silica xerogel was prepared by sol-gel process using tetraethylorthosilicate (TEOS), distilled water methanol and nitric acid in the volume ratio of 16:10:70:04 respectively, cadmium nitrate and thiourea are used as cadmium and sulfur sources. Silica gel containing 0.1 M of $Er^{3+}$ with and without CdS were prepared by sol-gel process with TEOS, as a precursor in the presence of methanol, water and nitric acid [22–24]. First, a desired amount of erbium oxide was dissolved in methanol and water in presence of nitric acid. Then to this mixture TEOS was added and stirred for 30 min. Second, the methanol solution of cadmium nitrate and thiourea was added into the above mixture and stirred. Cadmium nitrate and thiourea were as cadmium and sulfur sources, respectively. After being stirred for 60 min, the mixture was poured into polyethylene container, seal tightly and gelatinized at room temperature. The xerogel obtained was aged for 24 days. Finally, the xerogel was annealed at 150 °C for 1 h. The color of the xerogel turned from white into yellow, which shows the presence of CdS in the sample.

## Characterization Techniques

The size of the particles was determined from TEM images, obtained using a JEM-2100 transmission electron microscope with operating voltage of 200 kV. For this analysis, the samples were prepared by making a clear dispersion in ethanol and placing a drop of solution on a carbon-coated copper grid. The solution was allowed to evaporate leaving behind the nanoparticles on the carbon grid.

The absorption spectra were measured using PD UV-VIS spectrophotometer (S-3100). The fluorescence spectra were measured using a Horiba Jobin Yvon FluoroMax-4P spectrofluorometer equipped with 100 W Xenon lamp source. All the spectra were measured at room temperature.

## Result and Discussion

### Structural Analysis of CdS Nanoparticles Doped in the Glasses

For structural analysis, we analyzed the samples through TEM, the photograph of TEM image with selective area electron diffraction (SAED) is shown in Fig. 1(a) & (b), respectively. An average particle size of 10 nm is found from TEM, which is consistent with the crystallite size of 8.1 nm calculated by the Scherrer equation as well as the particles size 4.8 nm calculated by EMA, reported in our earlier paper [23, 24]. SAED pattern is used to learn about the crystal properties of a particular region i.e. the material is single crystalline, polycrystalline, polycrystalline textured or amorphous [25]. The SAED pattern of single crystalline materials have only spot patterns while polycrystalline materials have ring pattern form. In SAED pattern, it shows a ring like pattern, which means prepared CdS doped sample is a polycrystalline materials.

### Absorption Spectra of $Er^{3+}$ with and without CdS Nanoparticles in Silica Glasses: Judd-Ofelt Analysis

Figure 2 shows the absorption spectra of $Er^{3+}$ codoped with and without CdS nanoparticles. The band assignment are also indicated in Fig. 2. The spectral intensities for the observed bands of these glasses that are often expressed in term of oscillator strength of forced electronic dipole transition have

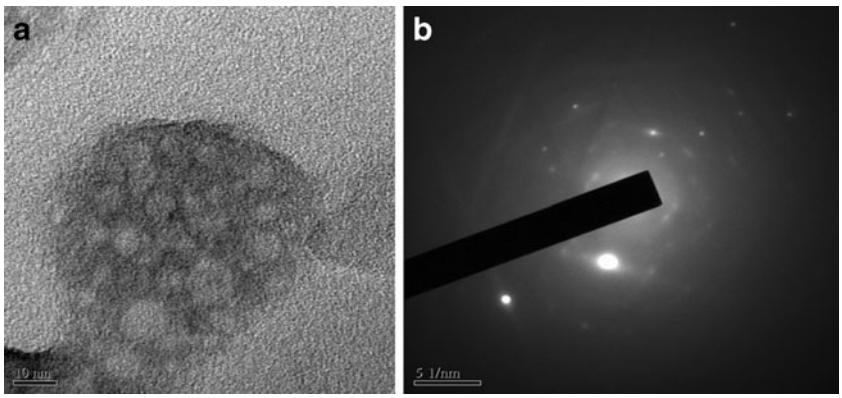


**Fig. 1** **a** TEM image of CdS nanoparticles doped in silica glasses **b** SAED pattern, Due to presence of rings with discrete spots confirm the larger grain size as well as polycrystalline nature

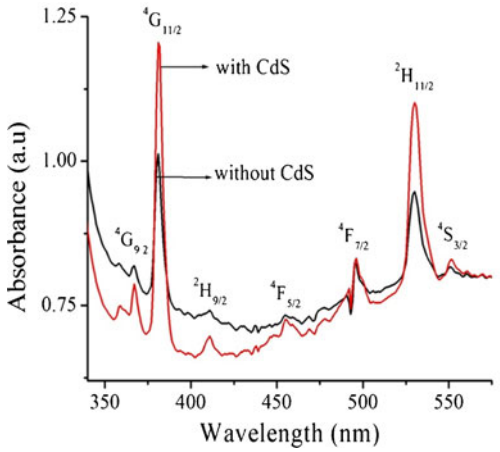


**Fig. 2** Absorption spectra of $Er^{3+}$ in sol-gel derived silica glasses

been analyzed with the help of Judd-Ofelt (J-O) theory [26, 27]. According to J-O theory, the oscillator strength of several $f—f$ transitions may be expressed by the sum of the product of three intensity parameter $\Omega_t$(t=2,4,6) times the squared matrix elements $\left\|U^{(t)}\right\|$ between the initial level $J$ to the terminal level $J'$ states. Once the phenomenological parameters for the rare-earth doped glass can be determined, it is used to predict the important radiative properties of the lanthanide ions in the host matrix. In the framework of the J-O theory, the theoretical oscillator strength $f_{cal}$ are expressed as a sum of the transition matrix element involving intensity parameters $\Omega_t$ which depends on the host matrix and is given by

$$f_{cal} = \left\{8\pi^2 mc\left(n^2+2\right)^2/3h\bar{\lambda}(2J+1)9n\right\} \times \sum_{t=2,4,6} \Omega_t |\langle J||U^{(t)}||J'\rangle|^2 \quad (1)$$

where $(2J+1)$ is the multiplicity of the lower states, $\bar{\lambda}$ is the mean wavelength of the transition, $c$ is the velocity of light, $m$ is the electronic mass, $h$ is the Planck's constant, $n$ is the refractive index and $\left\|U^{(t)}\right\|$ is the reduce matrix elements between the initial and terminal level. The $\Omega_t$ phenomenological parameters ($\Omega_t$) in Eq. (1) are determined from optical data for a particular ion-host combination.

The experimental values of oscillator strength $f_{exp}$ of the transition were evaluated from integrating absorbance for each band and the relation is

$$f_{exp} = 4.32 \times 10^{-9} \int \varepsilon(v)dv \quad (2)$$

where $\varepsilon$ ($v$) is the decadic molar extinction co-efficient at wave number $\bar{v}$ $cm^{-1}$ and is expressed as $\upsilon = a_v/2.303$, $a_v$ expressed the probability of absorption per unit time per unit concentration per unit length of optical path, from Lambert-Beer law.

The phenomenological intensity parameters $\Omega_t$($t$=2, 4, 6) for the forced electronic dipole transitions were obtained by using MatLab software in the framework of the J-O theory. The reduced matrix elements obtained by Carnall et al. [28] and refractive index ($n_d$)=1.514 for the sol-gel glass were employed in the calculations. The glass refractive index used in this was determined on a precision refractometer using a sodium vapour lamp with monobromonapthalene as the layer of contact between the glass surface and the refractometer prism. The experimental ($f_{exp}$) and calculated oscillator strength ($f_{cal}$) along with the root mean square deviation is compiled in Table 1. The J-O intensity parameters ($\Omega_t$) of $Er^{3+}$ doped glasses are compared in the Table 2.

The J–O parameters are important for investigating the local structure and bonding in the vicinity of the rare earth ions. The J–O parameter $\Omega_2$ is very sensitive to the structure and it is associated with the symmetry and covalency of the lanthanide sites. On the other hand, $\Omega_4$ and $\Omega_6$ values depend on the bulk properties such as viscosity and dielectric of the media and are also affected by the vibronic transition of the rare earth ions bond to the ligand atoms. In addition, the J–O intensity parameters can be used to calculate the spectroscopic quality $\frac{\Omega_4}{\Omega_6}$ that is critically important in predicting the stimulated emission for the laser active medium. Comparatively higher value of $\Omega_2$ parameter for studied glasses indicates the higher asymmetry and stronger covalent environment between $Er^{3+}$ and ligand ions for the studied host. The result is important since the transition probabilities for emission of $Ln^{3+}$ ions are expected to increase with increasing the covalency of the ions [29].

These $\Omega_t$ values have been used in the evaluation the strength of any radiative transition for any dopant and host combination from the observed photoluminescence spectra (PL). The electric dipole probability, which corresponds to the probability of spontaneous emission from an excited

**Table 1** Oscillator strength of $Er^{3+}$ co-doped with CdS nanoparticles in sol-gel silica glasses

| Transition from $^4I_{15/2}$ | Wavelength (nm) | Energy ($cm^{-1}$) | $f_{exp.}$($f_{exp}\times10^{-6}$) | $f_{cal}$($f_{exp}\times10^{-6}$) |
|---|---|---|---|---|
| $^4G_{9/2}$ | 367 | 27,248 | 0.3993 | 0.1204 |
| $^4G_{11/2}$ | 381 | 26,247 | 1.6293 | 1.5229 |
| $^2H_{9/2}$ | 411 | 24,331 | 0.6304 | 0.6376 |
| $^4F_{5/2}$ | 455 | 21,978 | 0.4710 | 0.5170 |
| $^4F_{7/2}$ | 496 | 20,161 | 0.4542 | 0.4713 |
| $^2H_{11/2}$ | 530 | 18,868 | 0.9597 | 0.9929 |
| $^4S_{3/2}$ | 551 | 18,149 | 0.4673 | 0.4227 |

**Table 2** Judd-Ofelt intensity parameters of $Er^{3+}$ doped in various glasses

| Host glass | $\Omega_2$ | $\Omega_4$ | $\Omega_6$ | $\frac{\Omega_4}{\Omega_6}$ | Reference |
|---|---|---|---|---|---|
| $Er^{3+}$/CdS | 14.1083 | 14.0638 | 11.4749 | 1.23 | Present work |
| Aluminate | 5.60 | 1.60 | 0.61 | 2.62 | [11] |
| Phosphate | 3.89 | 1.01 | 0.55 | 1.84 | [12] |
| Tellurite | 5.05 | 1.45 | 1.22 | 1.19 | [13] |
| Fluoride | 2.91 | 1.27 | 1.11 | 1.13 | [13] |

state, can also be determined through the knowledge of the transition strength, which is given by

$$A[(S,L)J;(S',L')J'] = \frac{64\pi^4 e^2 n}{3h(2J+1)\bar{\lambda}^3}\frac{(n^2+1)^2}{9} \sum_{t=2,4,6}\Omega_t\left|\langle (S,J)J||U^{(t)}||(S',L')J'\rangle\right|^2 \quad (3)$$

Equation (3) can be used to estimate the radiative spontaneous lifetime for an excited state by simply summing the electric dipole probabilities corresponding to all of the possible transitions originating from the excited state. The radiative lifetime of an excited state can then be written as:

$$\frac{1}{\tau_{rad}} = \sum_j A_{i,j} \quad (4)$$

Finally the peak emission cross-section ($\sigma_p$) between an initial manifold $|(S,L)J\rangle$ to a final manifold $|(S',L')J'\rangle$ is given as

$$\sigma_p(\lambda_p) = \frac{{\lambda_p}^4}{8\pi c n^2 \Delta\lambda_{eff}} A[(S,L)J;(S',L')J'] \quad (5)$$

where n is the refractive index at the $\lambda_p$ peak fluorescence wavelength, $\Delta\lambda_{eff}$ the effective bandwidth and $c$ is the velocity of light.

## PL Studies of $Er^{3+}$ Codoped with CdS Nanoparticles in Silica Glass

The fluorescence spectra of $Er^{3+}$ codoped with different concentration CdS nanoparticles are shown in Fig. 3. We have observed only one emission peak at 534 nm due to $^2H_{11/2}\rightarrow{}^4I_{15/2}$ transition of $Er^{3+}$ ions. Using the J-O parameters obtain from absorption spectra we have calculated the values of radiative parameters for the observed transition in our glass, which is compiled in the Table 3. It was also observed that the emission intensity considerably increase with varying the concentration of CdS nanoparticles in the host. The possible explanation is that CdS nanoparticles doped in the network of $SiO_2$-$Er^{3+}$ xerogel would increase

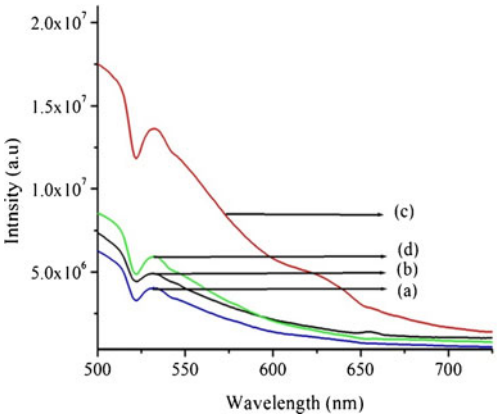


**Fig. 3** PL spectra of $Er^{3+}$ doped with CdS nanoparticles in silica glasses, a) without CdS, b) 0.1 M CdS, c) 0.3 M CdS & d) 0.5 M CdS

the concentration of Si dangling and oxygen vacancy in the network of the silica xerogel. In this way, more electron or hole can be easily excited and radiant recombinations are increased. Also, there is a possibility of ET from the CdS nanoparticles to the RE ions, owing to the electron or hole trapped surface levels. The photogenerated electron is first trapped in the surface level of CdS particles, they interact with the RE ions located close to the surface CdS. Secondly, the electron in the surface trapped recombines with a valence band free hole, and the energy is non-radiatively transferred to the RE ions.

## UC Studies of $Er^{3+}$ Codoped with CdS Nanoparticles in Silica Glass

Figure 4 illustrated the upconversion spectra of $Er^{3+}$ doped CdS nanoparticles in sol-gel silica glasses under 800 nm excitation. The emission bands were observed around 534, 560, and 680 nm. They are assigned to radiative transitions from the state's 7 to 1 ($^2H_{11/2}\rightarrow{}^4I_{15/2}$) from 6 to 1 ($^4S_{3/2}\rightarrow{}^4I_{15/2}$), and from 5 to 1 ($^4F_{9/2}\rightarrow{}^4I_{15/2}$), respectively. It was also observed the upconversion emission intensity varies with varying concentration of CdS nanoparticles. The possible explanation is that CdS nanoparticles doped into the network of $SiO_2$-$Er^{3+}$ xerogel would increase the concentration of Si dangling and oxygen vacancy in the network of silica xerogel. In this way, more electron and hole can be easily excited and radiant recombination are increased. Moreover, there is a possibility of energy transfer

**Table 3** Transition probabilities, radiative lifetime and peak emission cross-section of excited states of $Er^{3+}$ doped CdS nanoparticles in sol-gel silica glass

| Transition | Wavelength (nm) | A($s^{-1}$) | $\tau_R$(ms) | $\sigma_p\times10^{-22}$ $cm^2$ |
|---|---|---|---|---|
| $^2H_{11/2}\rightarrow{}^4I_{15/2}$ | 534 | 426.847 | 2.343 ms | 18.40 |

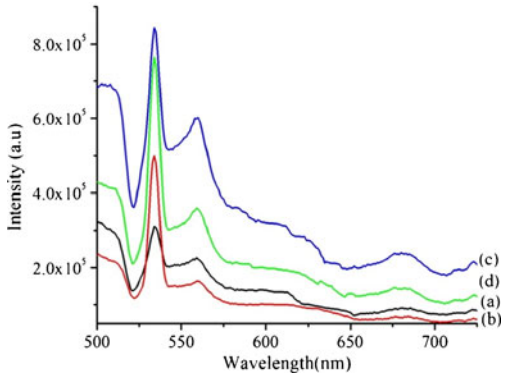


**Fig. 4** UC spectra of $Er^{3+}$ doped with CdS nanoparticles in silica glasses, a) without CdS, b) 0.1 M CdS, c) 0.3 M CdS & d) 0.5 M CdS

from CdS nanoparticles to $Er^{3+}$ ions in the matrix. As a result of this, the emission intensity of the doped sample markedly increased.

The possible upconversion mechanism in our samples can be explained with the help of energy level diagram shown schematically in Fig. 5. In the first step, the $^4I_{9/2}$ level is directly excited with 800 nm light, the initial $^4I_{9/2}$ level population relax to the $^4I_{11/2}$ & $^4I_{13/2}$ levels, with part of population in the $^4I_{11/2}$ level further relax into the $^4I_{13/2}$ level. With this excitation condition, the excited state absorption (ESA) process from the $^4I_{13/2}$ level to the $^2H_{11/2}$ level can occur easily in the system. Certainly the energy transfer(ET) through $^4I_{11/2}$ and the ESA from the $^4I_{11/2}$ should also considered, but contribution are smaller than the ESA from the $^4I_{13/2}$ level. This populates the $^2H_{11/2}$ level, from which it radiatively relax to $^4I_{15/2}$ level. Thus upconversion emission at 534 nm could be observed. Moreover, $Er^{3+}$ ion at the $^2H_{11/2}$ state can also decay to the $^4S_{3/2}$ state due to multiphonon relaxation process and the $^4S_{3/2}\rightarrow{}^4I_{15/2}$ transition gives 560 nm emission. The estimated

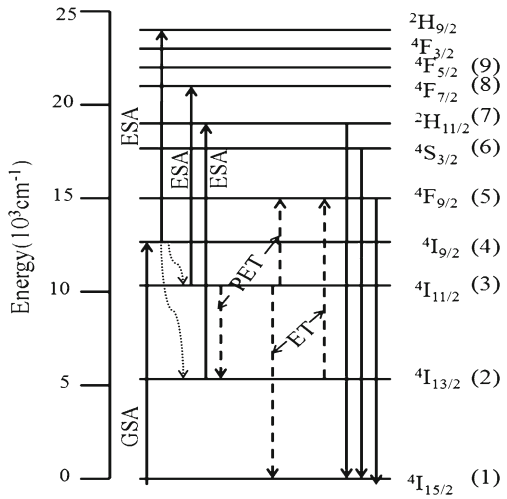


**Fig. 5** Energy level scheme for $Er^{3+}$ ions indicating possible upconversion mechanism

energy gap between the $^2H_{11/2}$ state and the next lower state $^4S_{3/2}$ is about 800 $cm^{-1}$. Thus the multiphonon relaxation is very large. The radiative transition from $^2H_{11/2}$ & $^4S_{3/2}$ to the ground state($^4I_{15/2}$) is responsible for the observed green band.

Finally, for the red upconversion under 800 nm excitation, the population of $^4F_{9/2}$ level is the combined result of ET from the $^4I_{13/2}$ level and the contribution from higher energy level by non-radiative relaxation. The ET process can be describe as

$$Er^{3+}\left(^4I_{13/2}\right)+Er^{3+}\left(^4I_{11/2}\right)\rightarrow Er^{3+}\left(^4F_{9/2}\right)+Er^{3+}\left(^4I_{15/2}\right)$$

and it is dominant contribution to red upconversion because the cross-relaxation should be due to high population of $^4I_{13/2}$ level. Moreover, $Er^{3+}$ ion was directly excited to the $^4F_{9/2}$ with phonon assistant energy transfer (PET) process from state $^4I_{11/2}$ to $^4F_{9/2}$. This combined process results to red upconversion emission at 680 nm due to transition from $^4F_{9/2}\rightarrow{}^4I_{15/2}$.

The rate equation used to describe the above mentioned process are given by

$$\frac{dn_1}{dt}=-W_{GSA}^{(1,4)}n_1(t)+\left[W_{ET}^{(2,5:3,1)}\frac{n_3(t)}{N}\right]n_2(t)+W_{EDT}^{(7,1)}n_7(t)+W_{EDT}^{(6,1)}n_6(t)+W_{EDT}^{(5,1)}n_5(t)$$

$$\frac{dn_2}{dt}=-\left[W_{ESA}^{(2,7)}+W_{ET}^{(3,1:2,5)}\frac{n_2(t)}{N}\right]n_2(t)+\left[W_{MPR}^{(4,2)}+W_{MPR}^{(3,2:3,5)}\frac{n_3(t)}{N}\right]n_3(t)$$

$$\frac{dn_3}{dt}=-\left[W_{ESA}^{(3,8)}+W_{PET}^{(3,2:3,5)}\frac{n_3(t)}{N}\right]n_3(t)+W_{MPR}^{(4,3)}n_4(t)$$

$$\frac{dn_4}{dt}=-\left[W_{MPR}^{(4,3)}++W_{MPR}^{(4,2)}+W_{ESA}^{(4,10)}\right]n_4(t)+W_{GSA}^{(1,4)}n_1(t)$$

$$\frac{dn_5}{dt}=\left[W_{PET}^{(3,2:3,5)}\frac{n_3(t)}{N}\right]n_3(t)+\left[W_{ET}^{(3,1:2,5)}\frac{n_2(t)}{N}\right]n_2(t)-W_{EDT}^{(5,1)}n_5(t)$$

$$\frac{dn_6}{dt}=W_{MPR}^{(7,6)}n_7(t)++W_{MPR}^{(8,6)}n_8(t)-W_{EDT}^{(6,1)}n_6(t)$$

$$\frac{dn_7}{dt}=W_{ESA}^{(2,7)}n_2(t)++W_{MPR}^{(8,7)}n_8(t)-W_{EDT}^{(7,1)}n_7(t)$$

Where $n_1$, $n_2$, $n_3$ … is the population of the state 1, 2, 3… etc. , N is the sum of the rare-earth concentration, $W^{(1,4)}$ denotes transition rates from 1 state to 4, similarly other too represent the same and $W_{ET}^{(2,5:3,1)}$ denotes energy transfer rates between two ions. These ions are in the state 2 and 3 before and in the state 5 and 1 after the transfer.

Ground state absorption rate ($W_{GSA}$) and excited state absorption rates ($W_{ESA}$) used in the rate equations are given by following equation [30]

$$W_{GSA} = \sigma\emptyset$$

$$W_{GSA} = \sigma'\emptyset$$

where $\sigma$ and $\sigma'$ denote absorption cross-section and Ø is a photon flux of the incident light.

Multiphonon relaxation rates ($W_{MPR}$) were approximately expressed in the following equation with the theory proposed by Miyagawa and Dexter [31]

$$W_{MPR} = Cexp(-\alpha\Delta E)$$

where $\Delta E$ is the energy gap to the next lower state. The parameters $C$ and $\alpha$ can be derived from the calculated electric dipole transition rate $W_{EDT}$, magnetic dipole transition rate ($W_{MDT}$) and the measured fluorescence lifetime [32].

And the phonon-assistant energy transfer rates ($W_{PET}$) can be expressed in the following equation [30]

$$W_{PET} = W_{ET}\exp(-\beta\Delta E)$$

$$\beta = \frac{\ln(2)}{h\upsilon} - \alpha$$

where $W_{ET}$ is the resonant energy transfer rate, $h\upsilon$ is a representative phonon energy in host glasses, and $\beta$ has correlation with $\alpha$ in multiphonon relaxation.

## Conclusion

In conclusion, the $Er^{3+}$ codoped with CdS nanoparticles in sol-gel glass with an average particle size of about 10 nm have been synthesized by sol-gel method. The upconversion of $Er^{3+}$ in CdS nanoparticles doped glasses has been investigated. The upconversion mechanisms are discussed, and the dominant mechanisms are ESA for the $^2H_{11/2}\rightarrow{}^4I_{15/2}$ and $^4S_{3/2}\rightarrow{}^4I_{15/2}$ transitions, and ET & PET for the $^4F_{9/2}\rightarrow{}^4I_{15/2}$ transition. Intense green ~ around 530–560 nm and red ~ around 680 nm emission bands were observed under 800 nm excitation.

**Acknowledgement** Authors wish to thanks Mr. Joston Nongkyrih, SAIF, NEHU for technical support in taking TEM micrograph. One of us (L. Bokatial) would like to thank the University Grant Commission (UGC) for the fellowship award.

## References

1. Yu H, Guo H, Zhang M, Liu Y, Liu M, Zhao L-J (2012) Distribution of $Nd^{3+}$ ions in oxyfluoride glass ceramics. Nanoscale Res Lett 7:275–288
2. R. Reisfeld, New materials for nonlinear optics, (1996) in: R. Reisfeld, C.K. Jorgensen (Eds.), Optical and Electronic Phenomena in Sol–Gel Glasses and Modern Applications, *Series: Structure and Bonding*, Vol. 85, Springer-Verlag, pp. 99.
3. Ehrhart G, Capoen B, Robbe O, Beclin F, Boy P, Turrell S, Bouazaoui M (2008) Energy transfer between semiconductor nanoparticles (ZnS or CdS) and $Eu^{3+}$ ions in sol-gel derive $ZrO_2$ thin film. Opt Mater 30(10):1595–1602
4. Zheng H, Gao D, Fu Z, Wang E, Lia Y, Tuan Y, Cui M (2011) Fluorescence enhancement of $Ln^{3+}$ doped nanoparticles. J Lumin 131(3):423–428
5. de Sousa DF, Zonetti LFC, Bell MJV, Ledullenger R, Hernandes AC, Nunesl LAO (1999) $Er^{3+}$: $Yb^{3+}$ codoped lead fluorindogallete glasses for min infrared and upconversion application. J Appl Phys 85:2502–2507
6. Higuchi H, Takahashi M, Kawamoto Y, Kadono K, Ohtsuki T, Peyghambarian N, Kitamura N (1998) Optical transition and frequency upconversion emission of $Er^{3+}$ ions in $Ga_2S_3$-$GeS_2$-$La_2S_3$. J Appl Phys 83:19–27
7. Kumar K, Rai SB, Rai DK (2006) Upconversion studies in $Er^{3+}$ doped $TeO_2$-$M_2O$(M = Li, Na and K). Solid State Comm 139 (7):363–369
8. Tsuda M, Soga K, Inoue H, Inoue S, Makishima A (1999) Upconversion mechanism in $Er^{3+}$ doped fluorozirconate glasses under 800 nm excitation. J Appl Phys 85:29–37
9. White JO, Mungan CE (2011) Measurement of upconversion in Er: YAG via Z-scan. J Opt Soc Am B 28(10):2358–2361
10. Li Y, Zhang J, Zhang X, Luo Y, Ren X, Zhao H, Wang X, Sun L, Yan C (2009) Near- infrared to visible upconversion in $Er^{3+}$ and $Yb^{3+}$ co-doped $Lu_2O_3$ nanocrystals: enhanced red color upconversion and three photon process in Green color upconversion. J Phys Chem C 113(11):4413–4418
11. Righini SC, Pelli S, Fossi M, Brenci M, Lipovskii AA, Kolobkova EV, Speghini A, Bettinelli M (2001) Characterization of Er-doped sodium-niobium phosphate glasses. Proc SPIE 4282:210
12. Tanabe S, Sugimoto N, Ito S, Handa T (2000) Broad-band 1.5 μm emission of $Er^{3+}$ ions in bismuth-based oxide glasses for potential WDM amplifier. J Lumin 87–89:670–672
13. Feng X, Tanaber S, Hanada T (2001) Spectroscopic properties and thermal stability of $Er^{3+}$ doped Germanotellurite glasses for broad band fiber amplifiers. Jn Am Ceram Soc 84(1):165–171
14. Freek Suijver J (2008) In: Ronda C (ed) Luminescence: From theory to application. WILEY-VCH Verlag GmbH & Co. KGaA, Weinheim, p 133
15. R. W. Boyed, (2008), Nonlinear Optics, Academic Press, 3rd Eds., Elsevier
16. Wang JS, Vogel EM, Snitzer E (1994) Tellurite glass: a new candidate for fiber devices. Opt Mater 3(3):187–203
17. Kumar VR, Reddy MR, Verraiah N (1995) Effect of DC field and X-ray irradiation on dielectric properties of $ZnF_2$-PbO-$TeO_2$. Phys State Sol (a) 147:601–610
18. Bokatial L, Rai S (2012) Photoluminescence and energy transfer study of $Eu^{3+}$ codoped with CdS nanoparticles in silica glasses. J Fluoresc 22:505–510
19. Baby Suganthi AR, Joshi AG, Sagayaraj P (2012) A novel two phase thermal approach for synthesizing CdSe/CdS core/ shell nanostructure. J Nanopart Res 14:691–700
20. Wang S, Li Y, Bai J, Yang Q, Song Y, Zhang C (2009) Characterization and photoluminescence studies of CdTe nanoparticles

before and after transfer from liquid phase to polystyrene. Bull Mater Sci 32(5):487–491
21. Kushwaha K, Gautom N, Singh P, Ramrakhaini M (2012) Synthesis and photoluminescence of CdSe/PVA nanocomposites. J Phys Conf Ser 365:012014
22. Rai S, Bokatial L (2011) Effect of CdS nanoparticles on photoluminescence spectra of $Tb^{3+}$ in sol-gel derived silica glasses. Bull Mater Sci 34:227–231
23. Rai S, Bokatial L, Dihingia PJ (2011) Effect of CdS nanoparticles on fluorescence from $Sm^{3+}$ doped $SiO_2$ glass. J Lumin 131:978–983
24. Bokatial L, Rai S (2010) Optical properties and upconversion of $Pr^{3+}$ doped CdS nanoparticles in sol-gel glasses. J Lumin 130:1857–1862
25. Goswami A (2007) Thin film fundamentals. New Age International Publishers, New Delhi, p 69
26. Judd BR (1962) Optical absorption intensities of rare-earth ion. Phy Rev 127:750–761
27. Ofelt GS (1962) Intensities of crystal spectra of rare-earth ions. J Chem Phys 37:511–520
28. Carnall WT, Fields PR, Rajnak K (1968) Electronic energy level in the trivalent lanthanide aquo ions. I. $Pr^{3+}$, $Nd^{3+}$, $Pm^{3+}$, $Sm^{3+}$, $Dy^{3+}$, $Ho^{3+}$, $Er^{3+}$ and $Tm^{3+}$. J Chem Phys 49:4424–4442
29. Ravi Kumar AV, Rao BA, Veeraiah N (1998) Dielectric properties of $LiF\text{-}B_2O_3$ glasses doped with certain rare earth ions. Bull Mater Sci 21:341–348
30. Chen CY, Petrin RR, Yeh DC, Sibley WA (1989) Concentration dependent energy transfer processes in $Er^{3+}$ and $Tm^{3+}$ doped heavy metal fluoride glasses. Opt Lett 14:432–434
31. Miyagawa T, Dexter DL (1970) Phonon sideband, multiphonon relaxation of excited state and phonon-assisted energy transfer between ion in solids. Phys Rev B 1:2961–2969
32. Shinn MD, Sibley WA, Drexhave MG, Brown EN (1983) Optical transition of $Er^{3+}$ ions in fluorozirconate glass. Phy Rev B 27:6635–6648